



# Electronic structure and linear optical property of $\text{BaSi}_2\text{N}_2\text{O}_2$ crystal

Lingli Wang\*, Haiyong Ni, Qihong Zhang, Fangming Xiao

Department of Rare Metals, Guangzhou Research Institute of Non-ferrous Metals, Guangzhou 510650, People's Republic of China

## ARTICLE INFO

### Article history:

Received 4 January 2011  
Received in revised form 11 August 2011  
Accepted 14 August 2011  
Available online 22 August 2011

### Keywords:

Oxonitride  
Electronic band structure  
Optical properties

## ABSTRACT

The electronic structure and linear optical property of  $\text{BaSi}_2\text{N}_2\text{O}_2$  (BSNO) have been calculated by density functional method with the local density approximation. A direct band gap of 5.17 eV at G is obtained for BSNO. The calculated total and partial densities of states indicate that the top valence band is mainly constructed from the N 2p and O 2p states, the low conduction band mostly originates from Ba 4d and Si 3p states. The calculated linear optical property of BSNO is in good agreement with the experimental measurement.

© 2011 Elsevier B.V. All rights reserved.

## 1. Introduction

Owing to the chemical and thermal stabilities, oxonitridosilicates have emerged as host lattices for highly efficient rare-earth doped luminescent materials applied in phosphor-converted (pc)-LEDs [1]. In recent years, the luminescence properties of  $\text{MSi}_2\text{N}_2\text{O}_2$  ( $M = \text{Ca}, \text{Sr}, \text{Ba}$ ),  $\beta\text{-SiAlON:Eu}$ , and  $\text{Ca-}\alpha\text{-SiAlON:Eu}$  have been investigated and particular promising properties have been pointed out [2–4]. Among them,  $\text{BaSi}_2\text{N}_2\text{O}_2\text{:Eu}^{2+}$  yields blue-green emission with a peak at 491 nm, which stands out due to its high quantum efficiency for UV-blue excitation (>60%), small Stokes Shift, narrow emission band and its low thermal quenching. Furthermore,  $\text{BaSi}_2\text{N}_2\text{O}_2\text{:Eu}^{2+}$  has a somewhat larger crystal field splitting, the low energy excitation band of  $\text{BaSi}_2\text{O}_2\text{N}_2\text{:Eu}^{2+}$  at unusual long-wavelength (400–450 nm) is expected [5,6]. Without the knowledge of the electronic structure of this compound, these distinguished luminescence properties cannot be understood profoundly.

In this paper, we present results of the plane wave density functional theory (DFT) calculation of the electronic structure and linear optical properties of BSNO. First-principle methods have been proved to be a powerful theoretical tool for acquiring accurate electronic levels and optical properties of metal compounds [7,8]. The present work attempts to theoretically characterize the band structure and the optical spectrum.

## 2. Methods and computational details

CASTEP [9,10], a plane-wave pseudopotential total energy package, is used for solving the electronic and band structures as well as linear optical properties of BSNO crystal. The theoretical basis of CASTEP is the density functional theory [11] approximation (LDA) developed by Kohn and Sham [12]. Within such a framework, the preconditioned conjugated gradient (CG) band-by-band method [10] used in CASTEP ensures a robust and efficient search of the energy minimum of the electronic structure ground state. The optimized pseudopotential [13,14] in the Kleinman–Bylander form [15] for Ba, Si, N, and O allows us to use small plane-wave basis sets without compromising the accuracy required by our study. The rather soft and optimized O pseudopotential has been tested in various systems [16], which enable us to use a kinetic-energy cutoff of 300 eV throughout the calculation. Its reliability will be further demonstrated in the results of the linear optical property calculation. The Read and Needs [17] correction is implemented to ensure accurate optical matrix elements calculations for our nonlocal pseudopotential based method.

In practice, the DFT calculated band gap is smaller than experimental result. This error is from the discontinuity of exchange-correlation energy. A 'scissors operator' is usually introduced, allowing a shift of the conduction bands to make the calculated result agree with the measured one [18,19]. The energy of 2.0 eV is selected for BSNO, which gives the best match between the theoretical value and experimental data.

## 3. Results and discussion

BSNO forms a complex orthorhombic structure with the space group of Pbcn [20]. As shown in Fig. 1, the structure of BSNO contains highly condensed  $\text{SiON}_3$  tetrahedral, the nitrogen atoms connect three silicon tetrahedral centers, while the oxygen atoms are terminally bound. The tetrahedras are connected by N atoms to form the sinoite  $\text{Si}_2\text{N}_2\text{O}$  layer. The  $\text{Ba}^{2+}$  ions are separated between these layers.

All these structural factors have their specific influence on the electronic structures and the optical properties of BSNO. An *ab initio* pseudopotential calculation can reveal the effects manifestly. With a real space atom-cutting method, the respective actions of

\* Corresponding author. Tel.: +86 20 61086469; fax: +86 20 37238536.  
E-mail address: [wll.bytt@163.com](mailto:wll.bytt@163.com) (L. Wang).

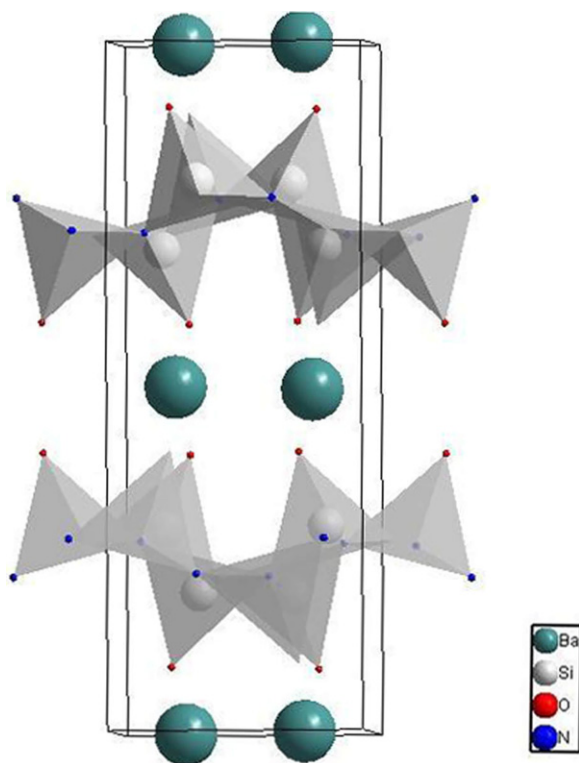


Fig. 1. Structure of BSNO crystal.

the anionic groups and cations on the electronic structure may be recognized and characterized.

The calculated band structure of BSNO along various symmetry lines is plotted in Fig. 2. The top of the valence band and the bottom of the conduction band are at G, with a direct gap of 5.17 eV. As we can see from Ref. [3], the absorption edge of BSNO is located at about 240 nm, and the host band gap is estimated to be 5.16 eV. The calculated result is consisted with the experimental one.

The total density of states (DOS) and partial density of states of BSNO crystal are shown in Fig. 3. In BSNO, the valence band is mostly composed of the 2p orbits of O and N atoms, while the conduction band is mainly constructed from the Ba 4d and Si 3p orbits. The calculated electronic structure indicates that the host absorption of BSNO occur not only in O–Ba but also in O–Si. So, the electron-transfer efficiency from the host to a doped rare earth atom is improved, and consistent with the high quantum efficiency of  $\text{BaSi}_2\text{N}_2\text{O}_2:\text{Eu}$  [3].

Fig. 4 represents the orbit-resolved PDOS of the various atoms. We can see that the energy bands are divided into five regions. The strongly localized state at  $-26$  eV is projected to be the Ba 5s orbit. The lower region around  $-17$  eV is mainly from the 2s orbits of O and N atoms. The region at about  $-11$  eV is composed of the 5p orbits of Ba atoms. The lower part of the valence band is constructed from N derived states and top valence band mainly consists of the O 2p orbits. The conduction band located at the upper region is mainly composed of the 4d orbits of Ba atoms and the 3p orbits of Si atoms.

The bonding picture can be more vividly illustrated by plotting the charge density maps of specific crystallographic planes. For BSNO crystal, we choose the best fit plane and the plane parallel to *b* and *c* axes. The calculated charge distribution in this plane is displayed in Fig. 5. As can be seen, the covalence of the Si–O bond and the Si–N bond within the  $\text{SiON}_3$  group is much strong and the Ba atom releases almost all its valence charge. These findings are direct

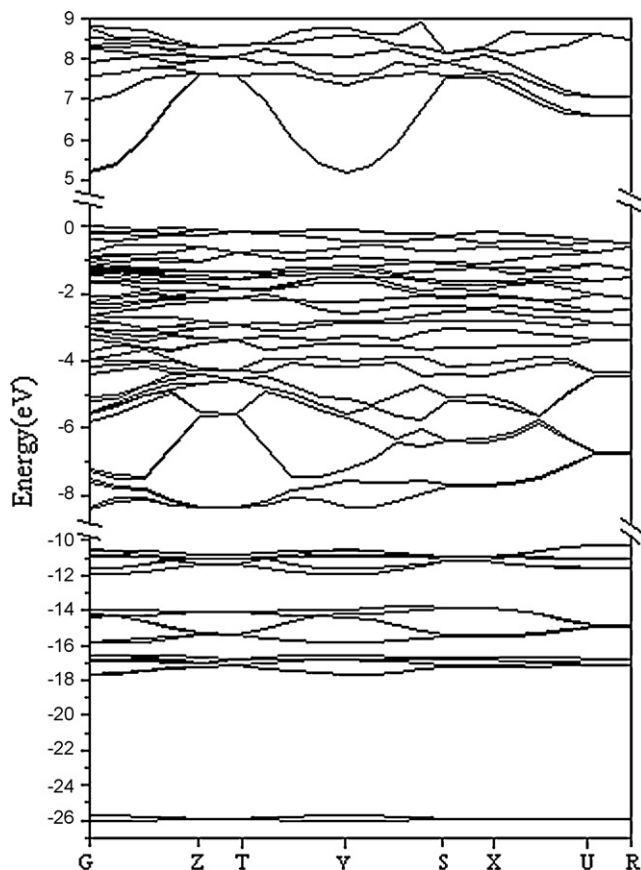


Fig. 2. Calculated band structure of BSNO.

consequences of the BSNO structure consisting of  $\text{SiON}_3$  forming a continuous network and barium atom lies in the mirror plane. The strong covalence of host is corresponding with the good thermal quenching behavior of  $\text{BaSi}_2\text{N}_2\text{O}_2:\text{Eu}$  phosphor.

Based on the calculated band structure, the linear Brillion domain (BZ) over independents 92  $\vec{k}$ -points is chosen for BSNO crystal to evaluate the momentum matrix elements of optical transitions. The calculated reflection spectrum of BSNO is plotted in Fig. 6. The absorption edge is located at about 240 nm, which is consistent with experimental result [6]. While the reflectance decreases more gradually than the experimental result. This may be from the error

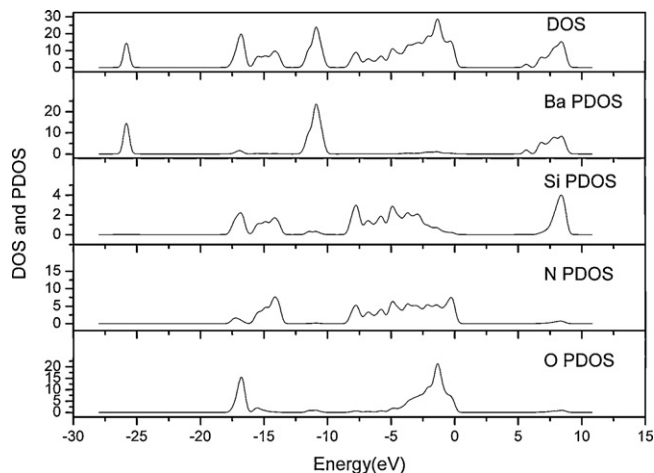


Fig. 3. Dos and PDOS plots of BSNO crystal.

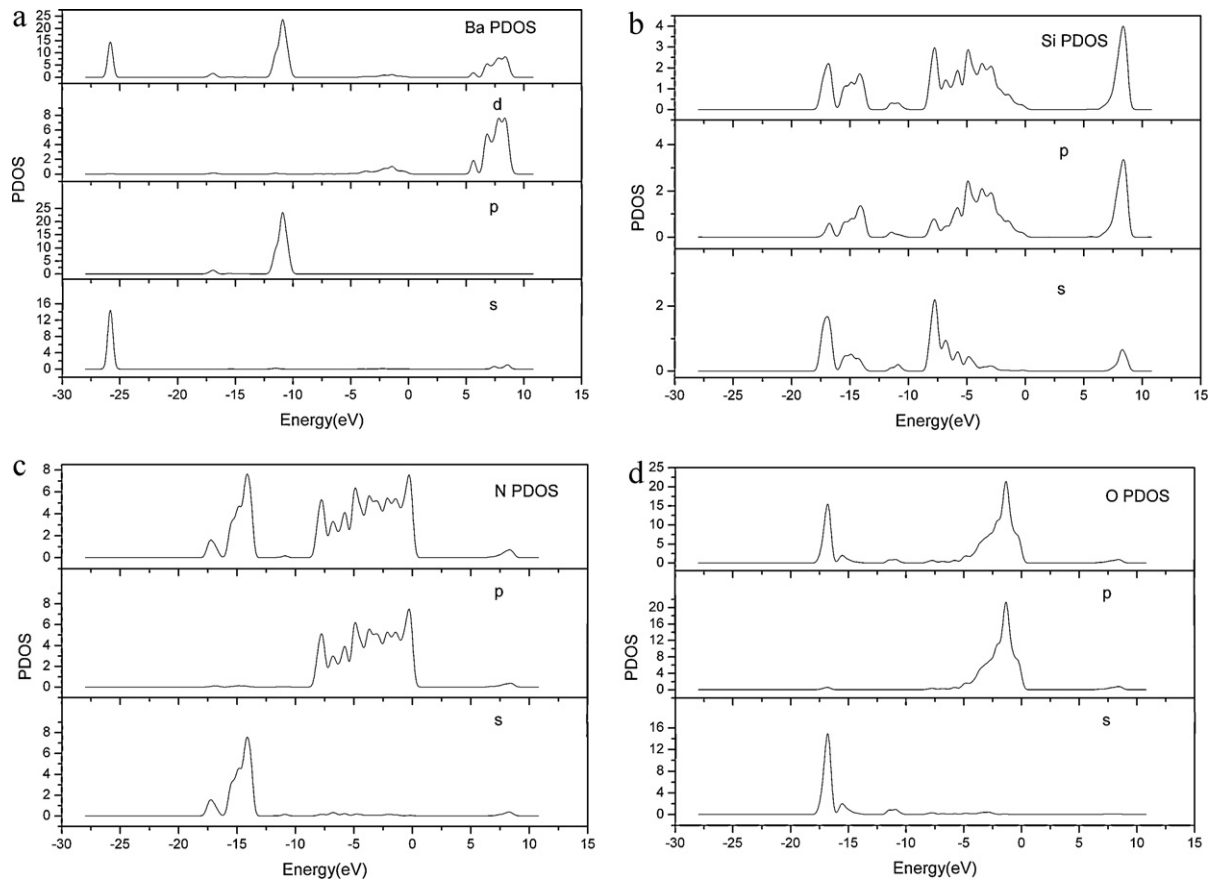


Fig. 4. Orbits-resolved PDOS of (a) Ba (b) Si (c) N and (d) O in BSNO.

of the calculation. As this crystal is excited, the absorption involves the O derived states as the initial states, the Si–O bond and Ba<sup>2+</sup> ion derived states as the final states. The inter-atomic transition in the (SiO<sub>3</sub>)<sup>7-</sup> group is weak, and the interatomic transition from O

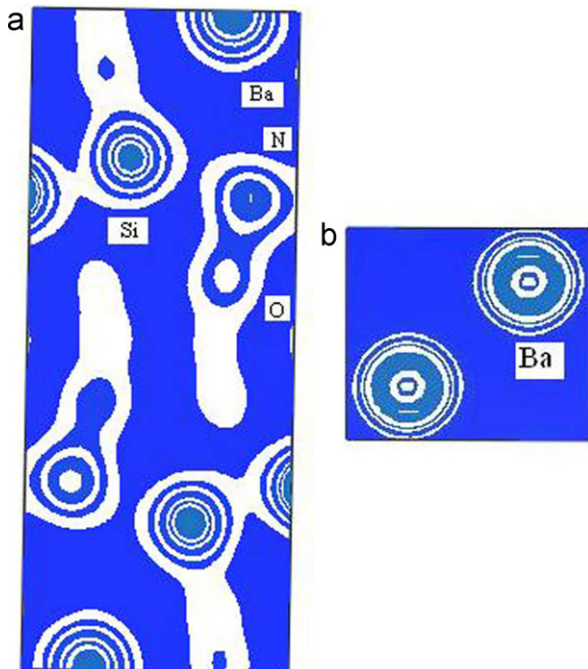


Fig. 5. The charge density of the best fit plane (a) and that of *b*–*c* plane (b).

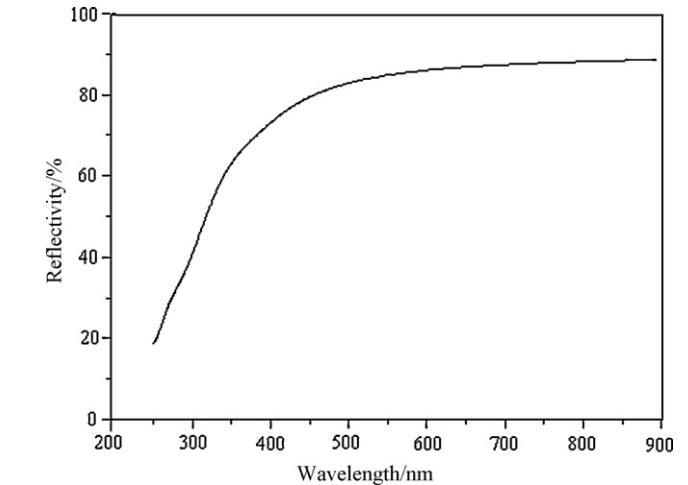


Fig. 6. Calculated reflection spectrum of BSNO crystal.

atoms to Ba<sup>2+</sup> ion is much strong. We deduce that the absorption of BSNO is dominated by the optical transition within the Ba–O band.

#### 4. Conclusions

The electronic structure and linear optical property of BSNO crystal have been calculated by means of the local-density-functional approach. The contributions of cations and anionic groups to the band structures are evaluated, respectively. The calculated absorption edge of BSNO agrees well with the experimental result, while the reflectivity is a little different. Nevertheless, these

results have provided an insight into the physical nature, which may be important to understand the energy transition process in this phosphor.

### Acknowledgements

This work was supported by Key Scientific Research Base of rare earth luminescent materials of Guangdong Province (2008A060303001) and Innovation fund of Guangzhou Research Institute of Non-ferrous Metals (2010A009).

### References

- [1] R. Mueller-Mach, G. Mueller, M.R. Krames, H.A. Höpfe, F. Stadler, W. Schnick, T. Juestel, P. Schmidt, *Phys. Status Solidi A* 202 (2005) 1727.
- [2] Y.Q. Li, A.C.A. Delsing, G. de With, H.T. Hintzen, *Chem. Mater.* 17 (2005) 3242.
- [3] R.-J. Xie, N. Hirotsaki, K. Sakuma, N. Kimura, *J. Phys. D: Appl. Phys.* 41 (2008) 144013.
- [4] K. Sakuma, N. Hirotsaki, R.-J. Xie, *J. Lumin.* 126 (2007) 843.
- [5] N. Kimura, K. Sakuma, S. Hirafune, K. Asano, N. Hirotsaki, R.-J. Xie, *Appl. Phys. Lett.* 90 (2007) 051109.
- [6] V. Bachmann, C. Ronda, O. Oeckler, W. Schnick, A. Meijerink, *Chem. Mater.* 21 (2009) 316–325.
- [7] Yu.S. Oseledchik, A.L. Prosvirnin, A.I. Pisarevskiy, V.V. Starshenko, V.V. Osadchuk, S.P. Belokry, N.V. Svitanko, A.S. Korol, S.A. Krikunov, A.F. Selevich, *Opt. Mater.* 4 (1995) 669.
- [8] K.C. Mishra, J.K. Berkowitz, B.G. DeBoer, E.A. Dale, *Phys. Rev. B* 37 (1988) 7230.
- [9] CASTEP 3.5 program developed by Molecular Simulations Inc., 1997.
- [10] M.C. Payne, M.P. Teter, D.C. Allan, T.A. Arias, J.D. Joannopoulos, *Rev. Mod. Phys.* 64 (1992) 1045.
- [11] P. Hohenberg, W. Kohn, *Phys. Rev. B* 136 (1964) 864.
- [12] W. Kohn, L.J. Sham, *Phys. Rev.* 140 (1965) A1133.
- [13] A.M. Rappe, K.M. Rabe, E. Kaxiras, J.D. Joannopoulos, *Phys. Rev. B* 41 (1990) 1227.
- [14] J.S. Lin, A. Qteish, M.C. Payne, V. Heine, *Phys. Rev. B* 47 (1993) 4174.
- [15] L. Kleinman, D.M. Bylander, *Phys. Rev. Lett.* 48 (1982) 1425.
- [16] (a) A. Takada, C.R.A. Catlow, J.S. Lin, G.D. Price, M.H. Lee, V. Milman, M.C. Payne, *Phys. Rev. B* 51 (1995) 1447;  
(b) I. Dawson, P.D. Bristowe, M.H. Lee, M.C. Payne, M.D. Segall, J.A. White, *Phys. Rev. B* 54 (1996) 13727;  
(c) M.H. Lee, C.F. Cheng, V. Heine, J. Klinowski, *Chem. Phys. Lett.* 265 (1997) 673.
- [17] A.J. Read, R.J. Needs, *Phys. Rev. B* 44 (1991) 13071.
- [18] C.S. Wang, B.M. Klein, *Phys. Rev. B* 24 (1981) 3417.
- [19] R.W. Godby, M. Schluter, L.J. Sham, *Phys. Rev. B* 37 (1988) 10159.
- [20] J.A. Kechele, O. Oeckler, F. Stadler, W. Schnick, *Solid State Sci.* 11 (2009) 537.